Pergamon

Geochimica et Cosmochimica Acta, Vol. 60, No. 16, pp. 3103–3113, 1996

0016-7037/96 $15.00 + .00

PII S0016-7037(96)00139-1

Thermal histories of IVA stony-iron and iron meteorites: Evidence for asteroid fragmentation and reaccretion

HENNING HAACK,[1,*] EDWARD R. D. SCOTT,[1] STANLEY G. LOVE,[1†] ADRIAN J. BREARLEY,[2] and TIMOTHY J. MCCOY[1‡]

[1]Hawai'i Institute of Geophysics and Planetology, School of Ocean and Earth Science and Technology, University of Hawai'i at Manoa, Honolulu, HI 96822, USA
[2]Institute of Meteoritics, Department of Earth and Planetary Sciences, University of New Mexico, Albuquerque, NM 87131, USA

(*Received May* 25, 1995; *accepted in revised form April* 24, 1996)

Abstract—We have investigated the thermal history of the IVA iron and stony-iron meteorites to help resolve the apparent conflict between their metallographic cooling rates, which are highly diverse, and their chemical trends, which favor crystallization in a single core. Transmission electron microscopy of the disordered clinobronzite in the stony-iron, Steinbach, using electron diffraction and high resolution imaging techniques indicates that this meteorite was rapidly cooled at ≈100°C/hr through 1200°C. The IVA irons cooled much slower in the range 1200–1000°C: absence of dendrites in large troilite nodules indicate cooling rates of <300°C/y. We infer that the parent asteroid was catastrophically fragmented and reaccreted when the core had cooled to 1200°C and was 95% crystallized. We argue that radiative heat losses from the debris cloud would have been minor due to its high opacity, small size (only a few asteroid diameters), and short reaccretion times (~ a few hours). We calculate that global heating effects were also minor (ΔT < 100°C for a body with a diameter of <400 km) and that the mean temperature of the IVA parent body before and after the impact was 450–700°C. We infer that Steinbach cooled rapidly from 1200°C at the edge of a core fragment by thermal equilibration with cooler silicates during and after reaccretion. Metallographic cooling rates of IVA irons and stony-irons for the temperature range 600–350°C (Rasmussen et al., 1995) strongly support this model and indicate that the IVA meteorites are derived from only a few core fragments. The large range of these cooling rates (20–3000°C/My) and the decrease in the metallographic cooling rates of high-Ni IVA irons with falling temperature probably reflect the diversity of thermal environments in the reaccreted asteroid, the low thermal conductivity of fragmental silicates, and the limited sintering of this fragmental material.

1. INTRODUCTION

Group IVA iron meteorites, which constitute the fourth largest group of irons with over fifty members, have chemical properties entirely consistent with fractional crystallization of an asteroidal core, but a wide range of metallographic cooling rates that appears to be inconsistent with a core origin (Moren and Goldstein, 1979; Rasmussen, 1982; Rasmussen et al., 1995). Other groups such as the largest and best studied group of irons, IIIAB, and the small group of Ni-rich irons, IVB, appear to have chemical properties and uniform metallographic cooling rates that are consistent with core origins (Haack and Scott, 1993; Rasmussen, 1989a,b). The silicate-bearing IAB and IIICD irons, which have been called nonmagmatic do not exhibit normal fractional crystallization behavior and have somewhat diverse cooling rates (Rasmussen, 1989b). They may have formed in impact-melt pools (Choi et al., 1995) or in S-rich cores (McCoy et al., 1993).

The apparent conflict between the interpretation of cooling rate and chemical data for group IVA has inspired many studies of these meteorites as both kinds of data provide important constraints on the geological history of asteroids and meteorites. Moren and Goldstein (1978, 1979) derived cooling rates of 4–200°C/My, which were inversely correlated with bulk Ni concentration and concluded that IVA irons formed at various depths inside a single body. Attempts to reconcile the conflicting cooling rate and chemical data by invoking fragmentation and reaccretion of core fragments seemed implausible to Scott (1979) as it would have required that the burial depth was correlated with composition. Rasmussen (1982) argued that low-Ni and high-Ni IVA members were derived from separate bodies, as proposed initially on the basis of kamacite bandwidth and Ni data by Schaudy et al. (1972). Rasmussen (1982) concluded that the large variation in metallographic cooling rates among low-Ni IVA ruled out a common core origin and suggested that these irons had been buried at different depths. Rasmussen et al. (1995) used a more recent phase diagram and diffusion rate data (Saikumar and Goldstein, 1988 and references therein) and analyzed more IVA meteorites. They found somewhat higher cooling rates in the range 20–3000°C/My with the low-Ni group showing fast, diverse cooling rates and the high Ni group showing slow and very similar thermal histories, consistent with cooling in the same thermal environment.

Chemical data for group IVA irons have been modeled

* *Present address:* Fysisk Institut, Odense Universitet, DK-5230 Odense M, Denmark.
† *Present address:* California Institute of Technology, Division of Geological and Planetary Sciences, Mail Code 252-21, Pasadena, CA 91125, USA.
‡ *Present address:* Code SN4, NASA Johnson Space Center, Houston, TX 77058, USA.

by Scott et al. (1996) who concluded that the IVA irons come from a single asteroidal core that fractionally crystallized. Differences between the chemical trends in groups IVA and IIIAB irons appear to result largely from lower concentrations of S in the former. The gross depletion of moderately volatile siderophile elements in group IVA was attributed to nebular rather than planetary processes by Scott et al. (1996).

Another source of information on the formation and evolution of the IVA parent body is provided by the two stony-irons, Steinbach and São João Nepomuceno, which contain abundant pyroxene-tridymite inclusions. Scott et al. (1996) found from their analyses and modeling that the metallic phases of Steinbach and São João Nepomuceno match the composition of the solids crystallizing from the IVA core after 50 and 80% crystallization, respectively. Also, the metallographic cooling rates of the two stony-irons are indistinguishable from those of IVA irons with similar Ni concentrations (Rasmussen et al., 1995). Scott et al. (1996) and Ulff-Møller et al. (1995) argued that the stony-irons formed at the core-mantle boundary though the origin of the silicates remains uncertain. Tridymite-pyroxene mixtures are not found in other meteorites.

Silicates in Steinbach are also anomalous because they appear to have been quenched from high temperature. Reid et al. (1974) studied the coexisting ortho- and clinobronzite in Steinbach using X-ray crystallography and concluded that the clinobronzite had formed by inversion during rapid cooling of protobronzite which had equilibrated with orthobronzite at ~1200°C. Although the clinoenstatite in Steinbach resembles that in the Norton County aubrite, which formed by shock induced transformation from orthoenstatite, Reid et al. (1974) rejected a shock origin for the Steinbach clinoenstatite because they found no evidence of shock and small but significant compositional differences between orthobronzite and clinobronzite. They concluded that cooling from 1200–700°C was much more rapid than during development of the Widmanstätten pattern in the 700–500°C range. Reid et al. (1974) did not quantitatively characterize the cooling rate, but concluded that the Steinbach silicates must have been quenched through 1200°C.

Quenching of Steinbach silicates was also favored by Ashworth and Barber (1976) and Ashworth (1980), who used electron microscopy to study ortho-clinopyroxene intergrowths in chondrites and achondrites (but not in Steinbach). Despite this support, the work of Reid et al. (1974) has not been considered in subsequent discussions of the thermal history and origins of IVA irons. This may be because the association of Steinbach with IVA irons was questioned, or because the proposed thermal history did not seem plausible, especially for a sample from deep within the parent body. As part of a major collaborative study of IVA irons, we have studied the microstructure of pyroxenes in Steinbach using electron microscopy as there is now little doubt that Steinbach and São João Nepomuceno formed close to the IVA irons. Our studies confirm the conclusion of Reid et al. (1974), that Steinbach cooled rapidly from 1200–700°C. We interpret the thermal history of the IVA irons and stony-irons to indicate that the IVA parent body was catastrophically broken by an impact event and that core and mantle fragments subsequently reaccreted.

Catastrophic fragmentation and reassembly events have been proposed to explain the thermal histories of other meteorites including the ordinary chondrites, the Shallowater enstatite achondrite, and the ureilites (Grimm, 1985; Taylor et al., 1987; Keil et al., 1989, 1994). Some constraints on asteroid disruption have been provided by experimental and theoretical studies (Davis et al., 1989; Fujiwara et al., 1989). To understand the evolution of the IVA body we have also investigated theoretical constraints on the breakup and reassembly of asteroids and the thermal history of the fragments during and after such events.

2. TECHNIQUES AND SAMPLES

Three grains of twinned clinopyroxene in Steinbach were selected for transmission electron microscope studies from a thin section (UH 231) prepared from material from the Bergakademie Freiberg (Scott et al., 1996). Cores 2.5 mm in diameter that contained the grains of interest were removed with an ultrasonic drill. Although the Canada balsam used in the original section could not be dissolved, after immersion in acetone for several days it was possible to remove the disk and attached Canada balsam using a razor blade. Slotted copper grids were glued over the grains of clinopyroxene and were prepared for transmission electron microscope studies by conventional ion-beam milling techniques using a Gatan ion beam mill. The Canada balsam was milled away satisfactorily during this process. Transmission electron microscopy was carried out on a JEOL 2000FX analytical transmission electron microscope operating at 200 kV.

3. RESULTS

Only one of the three clinobronzite grains in Steinbach that was selected for study in the electron microscope could be tilted to orient the electron beam parallel to the (100) plane, the twin plane. TEM observations show that this grain is largely free of dislocations, indicating low shock levels, but otherwise has an extremely heterogeneous microstructure. Some domains (2–3 μm in size, measured along the a direction) consist of clinobronzite polysynthetically twinned on (100), with only minor evidence of disordering (Fig. 1a). Electron diffraction patterns from these regions show diffraction maxima due to the presence of the twins, and only minor streaking parallel to a*. A continuum of microstructures were observed in this grain from ordered clinopyroxene to regions that show a highly striated microstructure consisting of a disordered intergrowth of clinopyroxene and orthopyroxene (Fig. 1b). The electron diffraction patterns from these highly disordered regions show strong diffraction maxima with a 1.8 nm repeat, consistent with the presence of orthopyroxene intergrown with clinopyroxene (inset in Fig. 1b). The (h00) orthopyroxene diffraction maxima are diffuse and strongly streaked parallel to a*, showing that the lamellae are extremely thin and do not diffract coherently.

We have measured the thickness of a large number of individual lamellae of clino and orthopyroxene from high resolution TEM images in order to estimate the proportion of the two phases present and establish the distribution of lamellae thicknesses. Based on the measurements, shown in Fig. 2, we estimate that the pyroxene grain now consists of about 40 vol% orthopyroxene. Orthopyroxene lamellae are

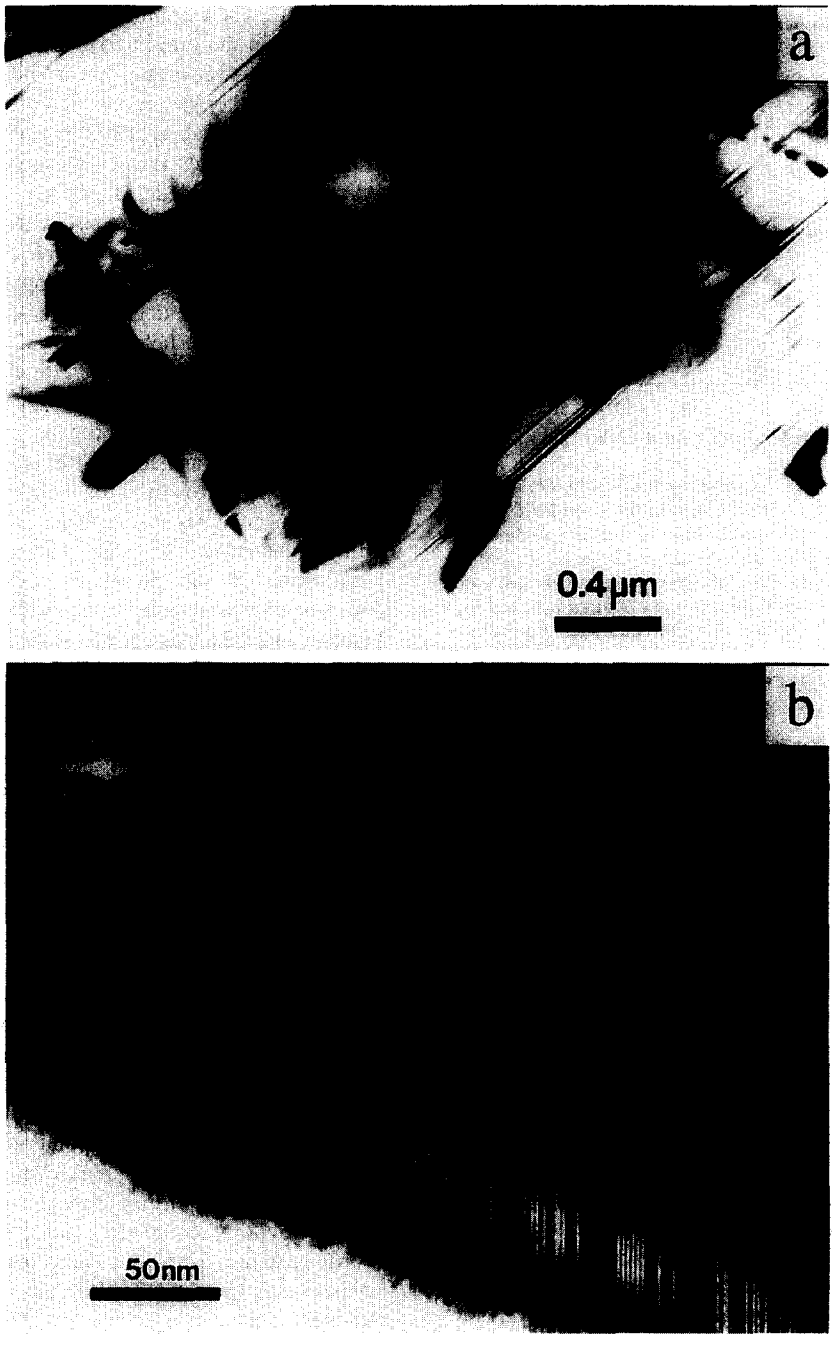

FIG. 1. Transmission electron microscope images of two regions in a twinned clinobronzite grain in the Steinbach stony-iron. (a) Bright-field electron micrograph showing polysynthetic twinning on (100). There is little evidence of disordering due to the presence of thin orthopyroxene lamellae intergrown with clinopyroxene. (b) High-resolution, bright-field lattice image of (100) planes in a moderately disordered region showing thin lamellae of orthopyroxene up to 5 unit cells in thickness (some examples are arrowed). The inset electron diffraction pattern shows strong streaking parallel to a* and (100) diffraction maxima with a 1.8 nm repeat from the orthopyroxene lamellae.

typically <10 unit cells in thickness, whereas clinopyroxene lamellae have a much broader range of thickness extending up to 50 unit cells in thickness. These distributions are typical of disordered low-Ca pyroxenes produced by rapid cooling through the temperature interval for the inversion of protopyroxene into orthopyroxene (Brearley and Jones, 1993).

4. DISCUSSION

4.1. Thermal History of the IVA Meteorites

4.1.1. Pyroxene microstructures

Three mechanisms for forming disordered low-Ca pyroxenes that are intergrowths of clinopyroxene and orthopyrox-

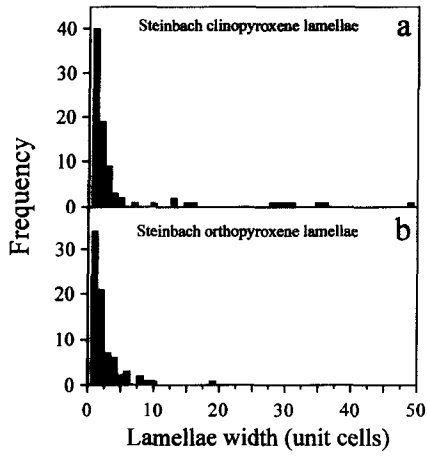

FIG. 2. Frequency distributions showing the widths of lamellae of (a) clinobronzite and (b) orthobronzite in the disordered clinobronzite grain in Steinbach shown in Fig. 1; lamellar widths are based on the unit cell repeat distance in the a direction: 0.9 nm in (a) and 1.8 nm in (b). The presence of clinopyroxene lamellae with widths that are odd and even multiples of the 0.9 nm repeat and the absence of orthopyroxene lamellae >20 unit cells wide are characteristic of disordered clinopyroxenes produced by rapid cooling of protopyroxene into the orthopyroxene stability field.

ene polymorphs are well established (e.g., Coe and Kirby, 1975; Buseck et al., 1982). These are (1) inversion from protoenstatite to form clinoenstatite during rapid cooling from high temperature, (2) inversion from orthoenstatite due to shear, either homogeneous or inhomogeneous (shock), and (3) annealing of clinoenstatite within the orthoenstatite stability field. A fourth mechanism has been proposed: annealing of orthopyroxene in a clinopyroxene stability field, but the existence of such a field is controversial.

The second and fourth mechanisms can be excluded because both produce clinopyroxene lamellae which have widths that are even multiples of the 0.9 nm repeat, unlike the lamellae in Steinbach, which have both odd and even multiples (Fig. 2a). The low abundance of dislocations and the existence of well-defined orthobronzite and disordered clinobronzite with different compositions, which are consistent with equilibration between orthopyroxene and protopyroxene at around 1200°C (Reid et al., 1974; Scott et al., 1996), confirm that the disordered clinopyroxene did not form from orthopyroxene by shock (Reid et al., 1974). The fractured nature of twinned clinopyroxene in Steinbach, which is like that observed in chondrules, is also consistent with formation from protopyroxene as this change involves a contraction of the crystal along the c-axis. Thus, the disordered clinobronzite in Steinbach formed either by rapid cooling of protopyroxene (mechanism 1) or by annealing of clinoenstatite formed by quenching (mechanism 3).

The first and third mechanisms can be distinguished from the microstructural details and the experiments of Brearley and Jones (1993). Brearley and Jones (1993) showed that the distribution of lamellae widths and the proportion of orthopyroxene are diagnostic of the cooling rate through the proto-to-ortho inversion temperature (≈1000°C for enstatite) and the total time between this temperature and about 600–700°C. Their preliminary studies of clinopyroxene annealed within the orthopyroxene stability field suggest that the transformation occurs by the formation of a few thick lamellae of orthopyroxene, which progressively coarsen. As a result, thick lamellae of orthopyroxene are more common in annealed samples than in those produced during monotonic cooling, provided that they have similar overall degrees of transformation. The presence in Steinbach of ortho lamellae which are dominantly <10 unit cells in width (Fig. 2b) and the overall abundance of orthopyroxene (40 vol%) preclude any significant degree of transformation by annealing in the orthoenstatite field.

We can estimate the cooling rate of Steinbach through the proto-orthopyroxene inversion interval from the dependence of the proportion of clinobronzite on the cooling rate, as given by Brearley and Jones (1993). Their data for enstatite suggest that intergrowths with 40 vol% orthoenstatite distributed heterogeneously (as in Steinbach) cooled at 100°C/hr, with an uncertainty of ~50°C/hr. For pyroxene with the composition of the Steinbach disordered clinopyroxene (Fs_{14}) the transition temperature is about 200°C higher. Since we can expect the transformation to be faster at higher temperatures, the cooling rate estimate of 100°C/hr at 1200°C is a lower limit, although further experiments are needed to confirm this.

To help understand how Steinbach could have cooled through 1200°C at 100°C/hr and about 10^{10} times slower at 500°C when kamacite formed, we discuss possible constraints from pyroxene microstructures on the time taken to cool from 900–600°C. Unfortunately, there is considerable uncertainty on the rate at which clinopyroxene transforms to orthopyroxene in this temperature range. Ashworth et al. (1984) annealed a disordered mixture of orthopyroxene and clinopyroxene from the Quenggouk H4 chondrite for a week at 800°C and completely transformed it to orthopyroxene. However, Brearley and Jones (1993) annealed synthetic pyroxenes and showed that the transformation rate is strongly dependent on the amount and nature of orthopyroxene initially present in the ortho-clino intergrowth. They found, for example, that annealing of pure clinoenstatite and clinoenstatite with 20 vol% orthopyroxene for 24 days at temperatures up to 980°C completely failed to transform any clino to orthoenstatite. Similarly, annealing of synthetic clinopyroxenes with Fs_{15} and $Fs_{15}Wo_1$ at 1045°C produced only extremely minor conversion of clino to orthopyroxene. Brearley and Jones (1993) infer that the transformation rate is highly dependent on the proportion of orthopyroxene initially present and the maximum width of existing orthopyroxene lamellae. Contrary to Ashworth et al. (1984), Brearley and Jones (1993) infer that disordered clinopyroxenes in Quenggouk were partly transformed to orthopyroxene by annealing inside an asteroid.

There are no studies of type 4–6 ordinary chondrites relating the degrees of clinopyroxene transformation during metamorphism to the metallographic cooling rates (1–1000°C/My) and maximum metamorphic temperatures (≈600–900°C). However, the evidence discussed above that Steinbach pyroxenes did not experience any significant degree of transformation from clino to orthopyroxene by annealing below 1200°C implies that the time spent by

Steinbach in cooling from 900 to 600°C was less than the time spent in this temperature interval by type 4–6 chondrites, which are partly or wholly transformed to orthopyroxene. It, therefore, seems likely that Steinbach spent less than 0.001–1 My in the temperature range 900–600°C.

4.1.2. Metal-troilite textures

Evidence for rapid cooling of Steinbach should also be preserved in the texture of metal-troilite intergrowths as a result of crystallization of Fe,Ni dendrites from trapped S-rich liquid below 1200°C. Dendrites that crystallized at a cooling rate of 100°C/hr would have a secondary arm spacing of ≈0.3 mm (Scott, 1982). Our Steinbach sections lack cm-sized troilite-metal nodules which should show dendrites with this secondary arm spacing. However, our sections of Steinbach do show mm-sized, troilite-coated, metal nodules that could well have cooled at the rate inferred above.

IVA irons that have escaped melting by blacksmiths and shock heating show no trace of metallic dendrites in troilite-rich regions. Rounded troilite nodules 1–20 mm in size are commonly enclosed within large taenite crystals (30 cm or more in size), testifying to slow cooling (Buchwald, 1975). Cooling rates from 1200°C to 1000°C are best constrained by the dimensions of the largest troilite nodules that have not experienced shock melting. Buchwald (1975) lists seven IVA irons with troilite nodules 1–2 cm across that have not been shock melted. It seems likely in these cases, that if dendrites with a secondary arm spacing of <5 mm had formed, they would still be visible. Dendrites of this size in chondrites were not obliterated during kamacite growth by the migration of troilite grain boundaries (e.g., Scott and Rajan, 1981). Thus, those IVA irons which contain troilite nodules 10–20 mm in size must have cooled at rates of <300°C/y. This is much slower than the cooling rate we calculate for Steinbach on the basis of the pyroxene microstructure. Since we find it unlikely that the cooling rate of Steinbach should have decreased from 100°C/hr at 1200°C to less than 300°C/y at 1000°C we infer that the cooling rates of the IVA irons and stony irons were diverse at high temperatures.

If we assume that the hot core fragments came in contact with colder silicate fragments after the breakup and reassembly event we can use the upper limit of the cooling rate to infer a minimum size of core fragments which cooled at <300°C/y. This constraint implies that these relatively slowly cooled IVA irons were part of iron masses >30 m across while cooling from 1200°C.

4.1.3. Metallographic cooling rates

Rasmussen et al. (1995) measured metallographic cooling rates for the two IVA stony-irons and fourteen IVA irons and found a very large range of cooling rates, 20–3000°C/My, indicating cooling in several different environments (Fig. 3). To reconcile these data with the chemical trends that indicate a single crystallization location for IVA meteorites (Scott et al., 1996), we suggest that the IVA body was broken up as the core cooled through 1200°C (corresponding to 95% crystallization) and then gravitationally buried at

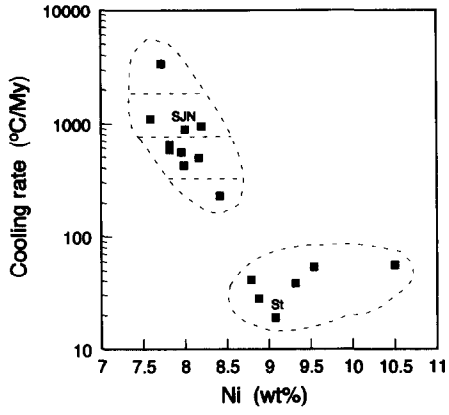

FIG. 3. Metallographic cooling rates of 16 IVA meteorites (data from Rasmussen et al., 1995). The two IVA stony-irons Steinbach (St) and São João Nepomuceno (SJN) have cooling rates which are indistinguishable from the IVA iron meteorites. Rasmussen et al. (1995) suggested that the large range of metallographic cooling rates indicated cooling in five different thermal environments.

diverse depth or in different thermal environments. Although the stony-irons seem to have cooled through 1200°C at much faster rates than the IVA irons, the cooling rates at 500°C appear to be indistinguishable from those of irons with comparable Ni concentrations (Fig. 3). Thus the breakup and reassembly event did not separate the IVA stony-irons from the IVA irons.

Because of the high thermal conductivity of metallic Fe,Ni, samples from a single metallic body should have cooling rates that are identical within experimental uncertainties. The high-Ni IVA irons (8.5–12 wt% Ni) have very similar thermal histories that are entirely compatible with cooling in a single metallic body. They cooled at 150°C/My in the temperature range 700–450°C and at 20°C/My below 450°C (Rasmussen et al., 1995). However, for the meteorites with <8.5 wt% Ni, Rasmussen et al. (1995) found that four separate locations are required to account for the range in metallographic cooling rates of 230–3000°C/My (Fig. 3).

Our IVA model (and almost all others that have been proposed) requires that the inverse correlation between Ni and metallographic cooling rate is a spurious correlation resulting from poor sampling of a small number of fragments. To calculate the probability of this occurrence we need to estimate the number of fragments that we have sampled.

One extreme view is that we have sampled meteorites with only two different cooling rates. In this case the apparent correlation is merely a result of a difference in cooling rate between a low-Ni and a high-Ni fragment. To derive all of the low-Ni IVA iron meteorites from the same fragment would, however, require the tenfold variation in cooling rates observed among these meteorites (Rasmussen et al., 1995) to be a result of analytical error (Fig. 3).

The other extreme is to assume that the we have sampled IVA iron meteorites from five different fragments (Rasmussen et al., 1995). With five fragments having different average Ni concentrations and cooling rates the probability of obtaining a correlation (positive or negative) by chance is

2/5! = 1/60. However, since fragment #1 in Rasmussen et al. (1995) is based on a single meteorite (Yingde) with a somewhat poorly defined cooling rate and fragments 2 and 3 have cooling rates that are only marginally different we believe that the number of sampled fragments could be as low as 3–4. The chance of obtaining a correlation by chance with three or four fragments is 1/3 or 1/12, respectively. A correlation based on three fragments is, therefore, not significant and a correlation based on four fragments only marginally significant. In view of the evidence for breakup and reassembly of the group IVA parent asteroid and the absence of any process that could produce a meaningful correlation between Ni concentration and cooling rate, we infer that the correlation is an artifact of sampling a small number of fragments (3–4) with diverse cooling rates and Ni concentrations.

Scott et al. (1973) inferred from histograms of Ni concentrations in group IIIAB and IVA, that we may have a representative compositional sample of group IVA. However, their IVA histogram and an updated version (Fig. 4) both show a dearth of IVA irons with Ni concentrations in the range 8.25–8.75 wt% implying that sampling may be poor. Schaudy et al. (1972) also noted this compositional gap and corresponding hiatus in kamacite bandwidth and suggested that high- and low-Ni IVA iron meteorites came from separate locations.

The large size of the parent taenite crystals in Steinbach and São João Nepomuceno, which can exceed 10 cm (Scott et al., 1996), also places constraints on their subsolidus thermal history. If the stony-irons had been quenched below 600–550°C, martensite would have begun to form (e.g., Wasson, 1974) rather than a fine-octahedral pattern. Reheating to >750°C would have converted the martensite back to taenite, but grain sizes could not have increased to 10 cm by recrystallization, especially given the constraint that there was no significant conversion of clinoenstatite to orthoenstatite as a result of annealing. Thus, Steinbach, and probably the IVA irons were not quenched below 600–550°C. However, it is possible that IVA irons may have been cooled relatively rapidly below the equilibrium exsolution temperature of kamacite (700–750°C).

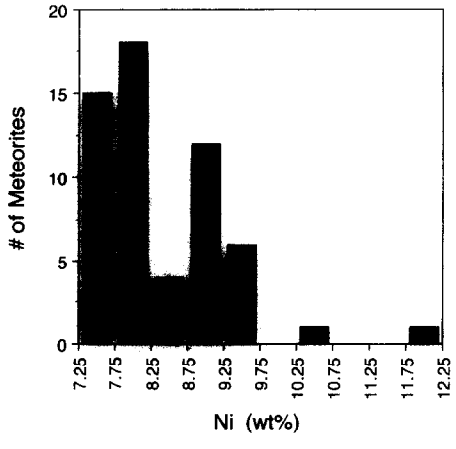

FIG. 4. Histogram showing abundance of IVA meteorites vs. Ni concentration. Note the dearth of IVA meteorites with Ni concentrations between 8.25 and 8.75 wt%. (Data are from Scott et al., 1996 and references listed therein).

4.1.4. *Summary*

The thermal and other constraints discussed above strongly suggest that Steinbach was quenched from 1200°C by catastrophic fragmentation of the group IVA parent body after 95% of the core had crystallized. We have not examined São João Nepomuceno in detail, but its similar ortho-clino intergrowth suggests that it had a high temperature thermal history similar to Steinbach. Prior to catastrophic fragmentation the stony-irons were probably located at the core-mantle boundary (Scott et al., 1996). The IVA irons and stony-irons are probably derived from a few core fragments that cooled through 500°C at diverse rates. Before we can infer more from the thermal history of the IVA meteorites, we need to understand how asteroids are broken up and reassembled.

4.2. Physics of Asteroid Collisional Breakup and Reassembly

High speed impacts can be characterized in terms of their specific energy (Q, projectile kinetic energy per unit target mass). At low Q the target is cratered but largely undamaged. An impact with specific energy above the shattering threshold (Q^*, defined when the largest fragment contains less than half of the original target mass) breaks the target into small fragments. We assume that Q^* for asteroids is ~1000 J/kg, following laboratory work using stony targets a few cm in size (Fujiwara et al., 1989). We also assume that asteroidal iron contains weak sulfur-rich regions between dendrites (Haack and Scott, 1992), making its toughness similar to that of stone. There is at least an order of magnitude uncertainty in scaling Q to asteroidal sizes and adjusting it for realistic materials (e.g., Fujiwara et al., 1989; Davis et al., 1994). The following discussion is therefore limited to very crude, order-of-magnitude accuracy.

Asteroids are held together by gravity as well as strength. The energy required to disperse the fragments of a shattered asteroid against their mutual gravity is the gravitational binding energy, $W = {}^3/_5\, GM^2/R$ for a homogeneous sphere, where G is the gravitational constant, M is the body's mass, and R is its radius. Dispersal requires that the fragments' kinetic energy exceed W. Not all of the impact energy is partitioned into target kinetic energy. Theory (e.g., O'Keefe and Ahrens, 1982; Melosh, 1989) and observations of impact craters (e.g., Grieve and Cintala, 1992) and asteroids (e.g., Davis et al., 1995) suggest that the fraction of projectile kinetic energy converted to target kinetic energy, η, is 0.1 to 0.4. The dependence of η on the size, geometry, relative velocity, and material properties of the collision partners is poorly understood. For this treatment, we assume that $\eta = 0.2$ with a factor of two uncertainty. It is also not known how the target kinetic energy is distributed amongst the many fragments. We assume here that all the fragments emerge at the same speed, a gross oversimplification which nonetheless may suffice given the current poor understanding of the problem (e.g., Davis et al., 1985, 1995; Fujiwara et al., 1989).

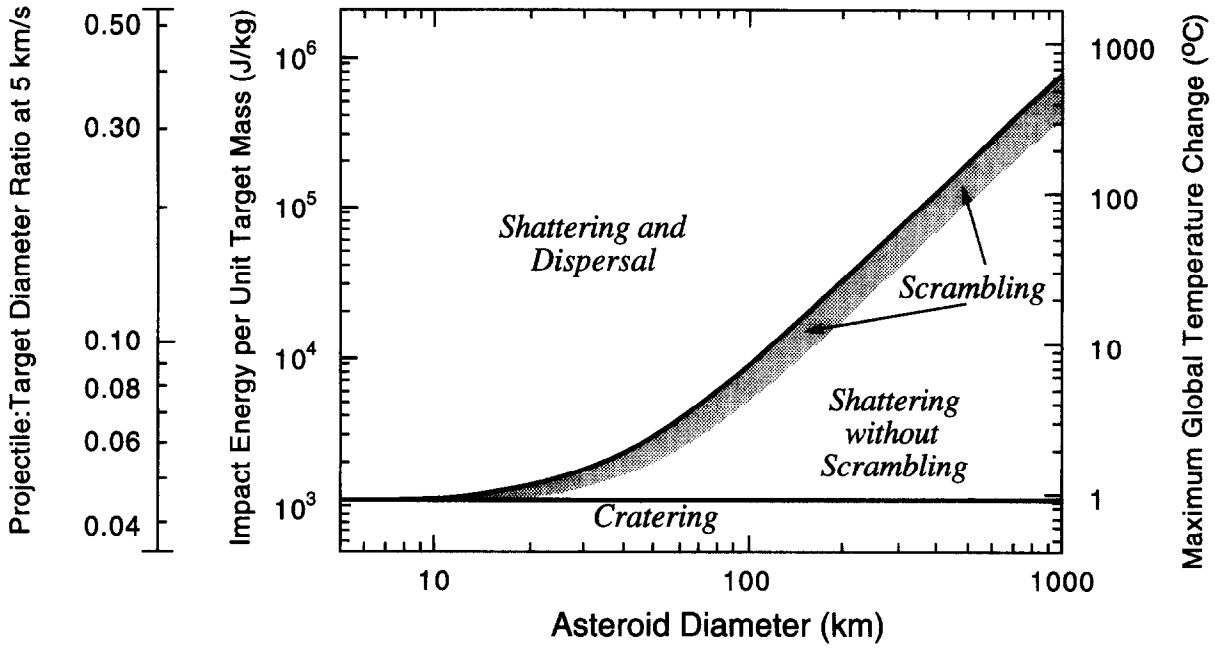

FIG. 5. Summary of the outcomes of impacts onto asteroids of different sizes. The horizontal axis is the target asteroid diameter in km; vertical axes are the specific energy of the impact, the corresponding projectile:target diameter ratio assuming collision partners of similar density and an impact speed of 5 km/s, and the temperature increase expected if all of the impact energy were converted to heat (assuming a heat capacity of 1200 J/kg/K), and distributed evenly throughout the target. The horizontal line near the bottom of the plot represents the (highly uncertain) shattering threshold: below the line, the asteroid is merely cratered; above the line the asteroid is shattered, or completely fractured throughout its volume. The slanted line, also highly uncertain, shows the energy required for dispersal of the fragments against gravity. Above the dispersal line, the impact shatters the asteroid and delivers enough kinetic energy to the pieces to disperse them. Immediately below the dispersal line is the energy window for launching, mixing, and reaccreting (scrambling) the target. In the portion of the chart below the dotted lower bound of the scrambling regime and above the shattering line, the impact shatters the asteroid but does not disperse the pieces, resulting in a rubble-pile structure with most fragments remaining near their original locations.

From these assumptions, we can guess the results of impacts onto asteroids of different sizes (Fig. 5). Note that bodies larger than ~30 km in diameter (with low escape velocties) have a growing range of the impact energies which result in shattering without dispersal of the fragments. In many such cases, most of the target material is broken up, but not significantly moved or mixed. Scrambling the target (launching, intermixing, and reaccreting the fragments) may require much more energy than shattering. Ejecting each fragment so that it could land at any point on the reaccreting debris pile requires launch speeds on the order of the asteroid's orbital velocity, which corresponds to a total debris kinetic energy about half the asteroid's gravitational binding energy. Using this guideline, we plot in Fig. 5 the energy window for scrambling the target. Because the number of projectile asteroids per (logarithmic) mass (M) bin varies (very approximately) as M^{-1} (Davis et al., 1994), a target with a large gap between Q^* and W might suffer ~2 scrambling impacts (with target ejecta energies ~ $W/2$) before it suffers a dispersing impact (target ejecta energy ~ W).

The minimum lifetime of the ballistic debris cloud is comparable to the orbital period at the asteroid's surface, or ~2 hours for any body of density 3.5 g/cm^3. Rare fragments lofted as far as the edge of the asteroid's gravitational sphere of influence (beyond which they would be lost into solar orbit) before falling back could reaccrete up to ~1 Earth year after the impact. The short interval between launch and reaccretion, along with the likelihood that the debris cloud is dusty and opaque, suggests that most fragments do not radiate away a significant amount of their internal heat during flight. Significant conductive heat transfer can occur between neighboring fragments of different temperature after reaccretion. The right-hand axis of Fig. 5 can be used to estimate the maximum global temperature increase an impact can cause without destroying the target. Only asteroids larger than several hundred km can suffer global heating of 100°C or more from a single impact.

In order to follow the thermal histories of core fragments during and after a breakup and reassembly event, we need to know the thermal profile in the IVA core and mantle immediately before the impact and the average temperature of the whole body.

4.2.1. *Average temperature of IVA body prior to impact*

Since we find that the radiative heat loss and impact heating released during breakup and reassembly are insignificant for small bodies (<400 km in diameter), the average temperature of the rubble pile after reassembly should be close to the average temperature of the body prior to the impact.

After reassembly, the hot core fragments will experience a period of enhanced cooling as they thermally equilibrate with the colder surrounding mantle rocks. Finally, slow cooling of the interior of the rubble pile will commence from the equilibration temperature. In order to study the low temperature thermal evolution of the IVA parent body we, therefore, need to determine the average temperature of the parent body prior to the breakup event.

We assume that breakup and reassembly occurred when Steinbach silicates were at 1200°C, the temperature at which orthopyroxene and protopyroxene equilibrated prior to quenching. (The precise temperature is not critical to this calculation.) Due to the much higher thermal conductivity of the metal core compared to the overlying silicate mantle, the core would have been almost isothermal (Haack et al., 1990). Thus to determine the average temperature, we need only the temperature profile through the mantle. Thermal models of cooling asteroids show that after the onset of core crystallization the temperature decreases linearly from the core-mantle boundary to the top of the mantle (Haack et al., 1990). The heat capacity of the core is approximately half the heat capacity of the mantle (600 and 1200 J K^{-1} kg^{-1}, respectively) but since the density of the core is approximately twice the mantle density the heat capacity per unit volume is very uniform through the asteroid. We can, therefore, calculate the average temperature as follows:

$$T_{ave} = \frac{1}{V}\int_0^R 4\pi r^2 T(r)dr = \frac{15T_{core} + 17T_{surf}}{32} \approx \frac{T_{core} + T_{surf}}{2}, \quad (1)$$

where the core is assumed to have a radius equal to half the total radius. V is the volume of the asteroid, R the total radius, T_{ave} the average temperature, T_{surf} the temperature at the surface of the asteroid, and T_{core} the temperature of the core. The surface temperature of the asteroid was probably close to −100°C. Assuming no regolith is present and a core temperature of 1200°C (based on Steinbach), we obtain a value of 550°C for the average temperature of the IVA parent body. Reducing the core mass from 25% to 10%, gives an average temperature of 420°C.

If an insulating regolith is present, the temperature at the top of the mantle should be used instead of T_{surf} in Eqn. 1 (Haack et al., 1990). Then the temperature at the top of the mantle could be raised significantly, but it is unlikely to exceed 525°C as this is the estimated sintering temperature (Wood, 1979; Yomogida and Matsui, 1984). In this extreme case, the average temperature of the body with a core mass of 25% would be 860°C. But during the early stages of the thermal evolution, volcanism would probably lead to sintering of any regolith present at the surface, so it is less likely that there was a substantial regolith present at the time of the inferred breakup. We estimate that the upper limit on the average temperature was around 700°C (corresponding to an upper mantle temperature of 200°C). Thus, our best estimate for the mean temperature of the IVA body at the time of impact is 450–700°C.

4.2.2. *Thermal history of asteroid debris*

We are now prepared to discuss the original goal of this treatment: how does collisional breakup and reassembly affect the thermal histories of meteorite samples derived from subsequent impacts? Specifically, what kind of cooling does a breakup/reassembly event impose on the interior of an asteroid with a hot core and cooler outer layers? Intuitively, we might guess that cooling could occur through two mechanisms: radiative cooling of internal rocks suddenly exposed to cold space or warmer debris, and conductive redistribution of thermal energy between asteroid fragments of different temperatures stirred together in the debris cloud and reaccreted side-by-side.

Radiative cooling to cold space is probably of minor importance. The catastrophic disruption of a large rocky body generates a prodigious quantity of dust. Theoretically and empirically, this is demonstrated by the steep slope of the power law describing fragment sizes ($n(s) = Cs^{-3.5}ds$) in collisional disruption experiments (e.g., Grün et al., 1985; Dohnanyi, 1978); intuitively, the catastrophic disruption of several cubic kilometers of a volcano in a major eruption, although not precisely analogous to the situation under consideration here, suggests that the environment of such an event is probably not optically transparent. Although the debris cloud's external radiative surface area may grow significantly, the opacity of the dust will prevent significant net loss of heat from the asteroid fragments by radiation to free space. Assuming a surface area of the debris cloud of four times the surface area of the asteroid and a surface temperature equal to the average temperature of the asteroid we can calculate the heat loss during a typical two hour flight time. The associated mean temperature drop is not likely to exceed 1°C even in the most favorably case (a 10 km radius asteroid with an average temperature of 700°C). We, therefore, infer that the total thermal loss of the asteroid during breakup was insignificant.

4.2.3. *Cooling rate of the Steinbach stony-iron*

If Steinbach crystallized at the core-mantle boundary as Ulff-Møller et al. (1995) conclude, the cooling rate of 100°C/hr at 1200°C that we derive suggests that Steinbach cooled in a meter-sized fragment or at an exposed surface of a larger fragment. The large proportion of pyroxene-silica intergrowths in Steinbach, which are totally absent in the IVA irons, suggests that Steinbach came from near a transition zone between metal and silicate. Since fractures are likely to propagate along surfaces where the material properties change abruptly, such as the core-mantle boundary (Greenberg and Chapman, 1983), it is plausible that an impact causing breakup and reassembly would make metal fragments with stony-iron surfaces. Such an origin appears to be consistent with the absence of shock effects in Steinbach. The constraint on the cooling rate of IVA irons at 1000°C (<300°C/y) implies that if the core was fractured as we suppose then the fragments were >30 m across. We infer that the cooling rate of core fragments would have been initially controlled by the debris cloud in which fragments were mixed and later by thermal equilibration and cooling of the reaccreted asteroid.

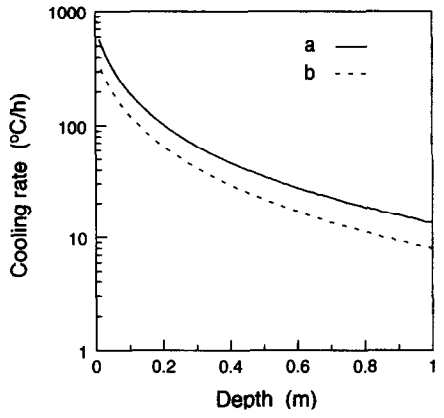

FIG. 6. Cooling rate at 1000°C as a function of depth for a metallic body cooling radiatively to backgrounds at −70°C (free space with sunlight, curve a) and 565°C (dust at the IVA asteroid's average internal temperature, curve b).

In the absence of firm constraints on the cooling rate of Steinbach at 1000°C, we assume that it cooled through 1000°C at the rate that we estimate for 1200°C: 100°C/hr. For comparison we calculate the cooling rate at 1000°C as function of depth for a fragment of metal initially at 1200°C that cools radiatively into various backgrounds. Irrespective of whether the background is at −70°C, free space with sunlight, or at 565°C, the mean temperature of the dense dust cloud that we infer enveloped the fragments, the cooling rate in the outermost 0.5 m is not significantly different from the Steinbach value (Fig. 6). The presence of hot dust and the short time of 2 hours available for radiative cooling would have ensured that little if any metal could have been quenched below the martensite formation temperature of 550–600°C.

4.2.4. *Physical setting of the IVA meteorites in the reassembled asteroid*

The metallographic cooling rates of IVA irons are entirely inconsistent with cooling inside a single asteroidal core but may be consistent with cooling inside a fragmented and reaccreted body. The one hundredfold range in the metallographic cooling rates (Moren and Goldstein, 1978, 1979; Rasmussen, 1982; Rasmussen et al., 1995) can be readily satisfied if thermal reequilibration of the core and mantle fragments and dust occurred after temperatures had dropped below 600–350°C, the critical range for the metallographic cooling rate technique. From our estimate of 450–700°C for the mean temperature of the reaccreted asteroid, we would infer that the core fragments were insulated from each other by large volumes of porous material. Although dust around the core fragments would have been sintered while temperatures fell to ~530°C (Wood, 1979), the much larger thermal capacity of the relatively colder mantle fragments and dust relative to that of the hot core fragments probably ensured that most dust was not sintered.

For a normal deeply buried iron meteorite that is undisturbed, we should not expect to detect any significant decrease in cooling through the temperature range that is critical for the metallographic cooling rate technique (600–350°C for IVA irons). But if IVA irons and stony-irons were part of hot core fragments that were mixed with mantle fragments of diverse but cooler temperatures, we should expect that some samples might show significant decreases in cooling rate in the temperature interval of 600–350°C. The decrease in metallographic cooling rate observed with decreasing temperature for the high-Ni IVA meteorites (Rasmussen et al., 1995) presumably results from thermal equilibration of the high-Ni core fragment with increasingly larger volumes of silicate (and metal, perhaps). Uncertainties in the initial thermal conditions in the asteroid, the size distributions of core and mantle fragments, and the complexity of the reaccreted mixture currently preclude any more detailed test of this model.

Cosmic-ray exposure ages for eight out of ten IVA irons

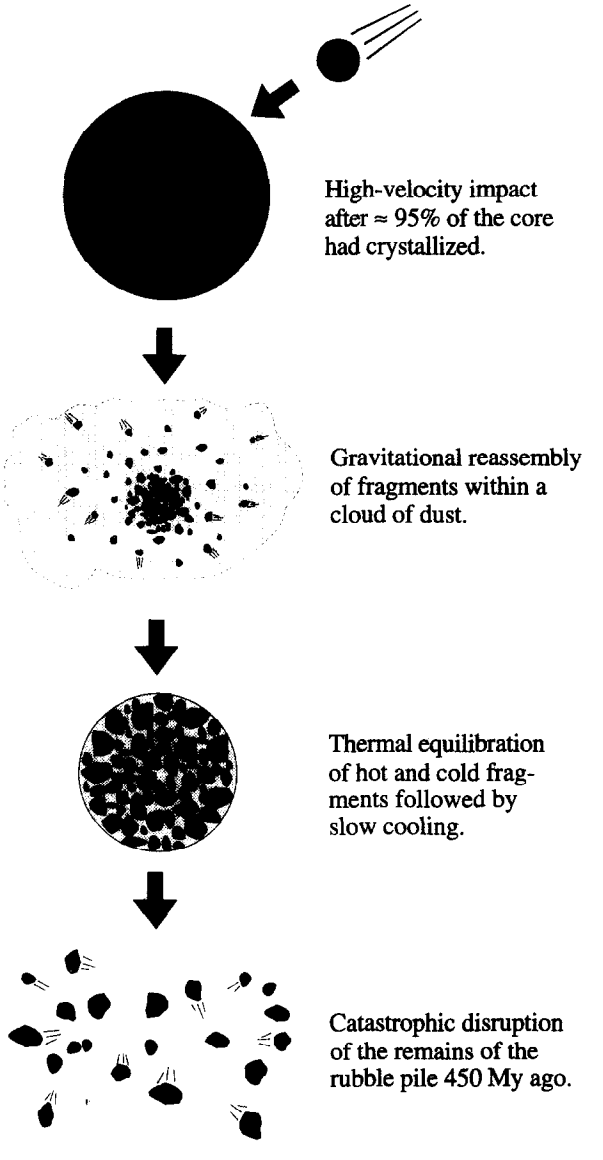

FIG. 7. Schematic representation of the four proposed stages in the evolution of the IVA parent body. Black is solid metal, white liquid metal, and grey is silicate.

are within error limits of 450 My (Voshage and Feldmann, 1979) suggesting that nearly all were ejected from the remains of their parent asteroid in what may have been a catastrophic impact (Keil et al., 1994). The two high-Ni IVA meteorites analyzed in this study, Hill City and Duchesne, have cooling rates like those of other high-Ni meteorites (Moren and Goldstein, 1979; Rasmussen et al., 1995). Their exposure ages of 475 ± 90 and 220 ± 70 My indicate that the core fragment (or fragments) that supplied high-Ni IVA meteorites was probably involved in the 450 My event. The 775 ± 50 My exposure age of the low-Ni IVA iron, Maria Elena, suggests that a few IVA irons were removed from the IVA body before 450 My ago.

We recognize two possible arguments against our proposed breakup and reassembly history for the IVA body. One, which we have already discussed, is the inverse correlation between Ni and cooling rate. We attribute this to poor sampling and predict that IVA meteorites will be discovered that violate this correlation; some may even lack the fine octahedral structure characteristic of IVA meteorites. Others may be discovered with mesosiderite like textures having formed when 5% of the core that was molten at the time of breakup and reassembly was mixed with cooler silicates.

The other possible argument against our model is the absence of achondritic meteorites from the mantle material that we infer to have been intermixed with the IVA core fragments in the reaccreted body. L and LL chondrites have oxygen isotopic compositions that match those of the IVA silicates (Clayton et al., 1983) but type 3–6 chondrites that cooled at a wide range of depth are unlikely to be derived from an asteroid that differentiated to form a metallic core. We infer from the absence of achondritic samples that the selection of silicate fragments from the 450 My impact which eventually became Earth-crossing were not large enough to survive the journey to Earth and were ground to dust within 100 My, the maximum cosmic-ray exposure age of ordinary chondrites.

5. SUMMARY

Chemical, chronological, and thermal data suggest that the IVA parent body suffered a breakup and reassembly event at a time when the core was mostly crystallized. We have used the above data to define the following stages in the evolution of the IVA parent body (Fig. 7).

1) *Igneous evolution of the IVA parent body ≈4.5 Gy ago.* The early evolution of the IVA parent body was probably not different from that of the parent bodies of the other groups of iron meteorites for which a core origin is inferred. After differentiation into mantle, core, and crust, cooling commenced and the core started to solidify. The stony-irons São João Nepomuceno and Steinbach may have formed somewhere near the core-mantle interface. When the core was mostly crystallized the parent body suffered a large impact that caused catastrophic fragmentation and reaccretion.
2) *Breakup and reassembly.* Large core fragments (>30 m in size) were mixed with cooler fragments from the mantle and crust. If Steinbach formed near the core-mantle boundary prior to breakup and reassembly, its rapid cooling rate of 100°C/hr at 1200°C probably reflects preferential fragmentation at the core-mantle boundary and mixing with cooler material. During the two hours necessary for most of the body to reaccrete, large amounts of dust produced in the impact would have minimized heat losses by radiation. Thus the average temperature of the rubble pile was close to the average temperature of the original body (450–700°C).
3) *Thermal equilibration of hot and cold fragments.* Thermal equilibration of hot core fragments and cooler mantle material at diverse depths ensured a unique range of thermal histories for the IVA samples. Some fragments buried at shallow depth maintained a high cooling rate throughout the temperature range where the Widmanstätten pattern forms. Other fragments, such as the source of the high-Ni IVA irons cooled relatively fast at high temperatures as they equilibrated with their colder surroundings. At lower temperatures, when the slow cooling of the entire rubble pile dominated, the cooling rate of the deeply buried fragments decreased.
4) *Dispersal of the rubble pile 450 My ago.* 450 My ago another high velocity impact dispersed the remains of the rubble pile. Samples from 3–4 of the core fragments that were formed in the breakup and reassembly event were shocked, reheated, and ejected into orbits that eventually became Earth-crossing. Silicate fragments with similar orbits were too small to survive 450 My of space erosion.

Acknowledgments—This work was supported in part by NASA grant NAGW 3281 (K. Keil, PI) and NAGW 3347 (J. J. Papike, PI). This is Hawaii Institute of Geophysics and Planetology publication No. 897, and School of Ocean and Earth Sciences and Technology publication No. 4104. Tove Nyberg is thanked for help in preparing the figures. Reviews from M. Miyamoto, J. I. Goldstein, A. M. Reid, and D. W. Mittlefehldt helped improve the manuscript. HH acknowledges support from the Danish Natural Science Research Council. Transmission electron microscopy was performed in the Electron Microbeam Analysis Facility, Department of Earth and Planetary Science, and Institute of Meteoritics, University of New Mexico.

Editorial handling: D. W. Mittlefehldt

REFERENCES

Ashworth J. R. (1980) Chondrite thermal histories: clues from electron microscopy of orthopyroxene. *Earth Planet. Sci. Lett.* **46,** 167–177.

Ashworth J. R. and Barber D. J. (1976) Shock effects in meteoritic pyroxene. In *Developments in Electron Microscopy and Analysis* (ed. J. A. Venables), pp. 517–520. Academic Press.

Ashworth J. R., Mallison L. G., Hutchison R., and Biggar G. M. (1984) Chondrite thermal histories by experimental annealing of Quenggouk orthopyroxene. *Nature* **308,** 259–261.

Brearley A. J. and Jones R. H. (1993) Chondrite thermal histories from low-Ca pyroxene microstructures: Autometamorphism vs prograde metamorphism revisited. *Lunar Planet. Sci.* **24,** 185–186.

Buchwald V. F. (1975) *Handbook of iron meteorites.* Univ. California Press.

Buseck P. R., Nord G. L., and Veblen D. R. (1982) Subsolidus phenomena in pyroxenes. *Rev. Mineral.* **7,** 117–211.

Choi B.-G., Ouyang X., and Wasson J. T. (1995) Classification and origin of IAB and IIICD iron meteorites. *Geochim. Cosmochim. Acta* **59,** 593–612.

Clayton R. N., Mayeda T. K., Olsen E. J., and Prinz M. (1983) Oxygen isotope relationships in iron meteorites. *Earth Planet. Sci. Lett.* **65,** 229–232.

Coe R. S. and Kirby S. H. (1975) The orthoenstatite to clinoenstatite transformation by shearing and reversion by annealing: Mechanism and potential applications. *Contrib. Mineral Petrol.* **52,** 29–56.

Davis D. R., Chapman C. R., Greenberg R., Weidenschilling S. J., and Harris A. W. (1985) Collisional evolution of asteroids: evidence from Vesta and Hirayama families. *Icarus* **62,** 30–53.

Davis D. R., Weidenschilling S. J., Farinella P., Paolicchi P., and Binzel R. P. (1989) Asteroid collisional history: effects on sizes and spins. In *Asteroids II* (ed. R. P. Binzel et al.), pp. 805–826. Univ. Arizona Press.

Davis D. R., Ryan E. V., and Farinella P. (1994) Asteroid collisional evolution: results from current scaling algorithms. *Planet. Space Sci.* **42,** 599–610.

Davis D. R., Ryan E. V., and Farinella P. (1995) On how to scale disruptive collisions. *Lunar Planet. Sci. Conf.* **26,** 319–320.

Dohnanyi J. S. (1978) Particle dynamics. In *Cosmic Dust* (ed. J. A. M. McDonnell), pp. 527–605. Wiley.

Fujiwara A. et al. (1989) Experiments and scaling laws on catastrophic collisions. In *Asteroids II* (ed. R. P. Binzel et al.), pp. 240–265. Univ. Arizona Press.

Greenberg R. and Chapman C. R. (1983) Asteroids and meteorites: Parent bodies and delivered samples. *Icarus* **55,** 455–481.

Grieve R. A. F. and Cintala M. J. (1992) An analysis of differential impact melt-crater scaling and implications for the terrestrial impact record. *Meteoritics* **27,** 526–538.

Grimm R. E. (1985) Penecontemporaneous metamorphism, fragmentation, and reassembly of ordinary chondrite parent bodies. *J. Geophys. Res.* **90,** 2022–2028.

Grün E., Zook H. A., Fechtig H., and Giese R. H. (1985) Collisional balance of the meteoritic complex. *Icarus* **62,** 244–273.

Haack H. and Scott E. R. D. (1992) Asteroid core crystallization by inward dendritic growth. *J. Geophys. Res.* **97,** 14727–14734.

Haack H. and Scott E. R. D. (1993) Chemical fractionations in group IIIAB iron meteorites: origin by dendritic crystallization of an asteroidal core. *Geochim. Cosmochim. Acta* **57,** 3457–3472.

Haack H., Rasmussen K. L., and Warren, P. H. (1990) Effects of regolith/megaregolith insulation on the cooling histories of differentiated asteroids. *J. Geophys. Res.* **95,** 5111–5124.

Keil K., Ntaflos Th., Taylor G. J., Brearley A. J., Newsom H. E., and Romig A. D. (1989) The Shallowater aubrite: evidence for origin by planetesimal impacts. *Geochim. Cosmochim. Acta* **53,** 3291–3307.

Keil K., Haack H., and Scott E. R. D. (1994) Catastrophic fragmentation of asteroids: evidence from meteorites. *Planet. Space Sci.* **42,** 1109–1122.

McCoy T. J., Keil K., Scott E. R. D., and Haack H. (1993) Genesis of the IIICD iron meteorites: evidence from silicate bearing inclusions. *Meteoritics* **28,** 552–560.

Melosh H. J. (1989) *Impact Cratering.* Oxford Univ. Press.

Moren A. E. and Goldstein J. I. (1978) Cooling rate variations of group IVA iron meteorites. *Earth Planet. Sci. Lett.* **40,** 151–161.

Moren A. E. and Goldstein J. I. (1979) Cooling rates of group IVA iron meteorites determined from a ternary Fe-Ni-P model. *Earth Planet. Sci. Lett.* **43,** 182–196.

O'Keefe J. D. and Ahrens T. J. (1982) The interaction of the Cretaceous/Tertiary extinction bolide with the atmosphere, ocean, and solid earth. *Geol. Soc. Amer. Spec. Pap.* **190,** 103–120.

Rasmussen K. L. (1982) Determination of the cooling rates and nucleation histories of eight group IVA iron meteorites using local bulk Ni and P variation. *Icarus* **52,** 444–453.

Rasmussen K. L. (1989a) Cooling rates of group IIIAB iron meteorites. *Icarus* **80,** 315–325.

Rasmussen K. L. (1989b) Cooling rates and parent bodies of iron meteorites from group IIICD, IAB, and IVB. *Physica Scripta* **39,** 410–416.

Rasmussen K. L., Ulff-Møller F., and Haack H. (1995) The thermal evolution of the IVA iron meteorites: evidence from metallographic cooling rates. *Geochim. Cosmochim. Acta* **59,** 3049–3059.

Reid A. M., Williams R. J., and Takeda H. (1974) Coexisting bronzite and clinobronzite and the thermal evolution of the Steinbach meteorite. *Earth Planet. Sci. Lett.* **22,** 67–74.

Saikumar V. and Goldstein J. I. (1988) An evaluation of the methods to determine the cooling rates of iron meteorites. *Geochim. Cosmochim. Acta* **52,** 715–726.

Schaudy R., Wasson J. T., and Buchwald V. F. (1972) The chemical classification of iron meteorites and its interpretation. VI. A reinvestigation of iron meteorites with Ge concentrations lower than 1 ppm. *Icarus* **17,** 174–192.

Scott E. R. D. (1979) Origin of iron meteorites. In *Asteroids* (ed. T. Gehrels), pp. 892–925. Univ. Arizona Press.

Scott E. R. D. (1982) Origin of rapidly solidified metal-troilite grains in chondrites and iron meteorites. *Geochim. Cosmochim. Acta* **46,** 813–823.

Scott E. R. D. and Rajan R. S. (1981) Metallic minerals, thermal histories and parent bodies of some xenolithic, ordinary chondrite meteorites. *Geochim. Cosmochim. Acta* **45,** 53–67.

Scott E. R. D., Wasson J. T., and Buchwald V. F. (1973) The chemical classification of iron meteorites-VII. A reinvestigation of irons with Ge concentrations between 25 and 80 ppm. *Geochim. Cosmochim. Acta* **37,** 1957–1983.

Scott E. R. D., Haack H., and McCoy T. J. (1996) Core crystallization and silicate-metal mixing in the parent body of the IVA iron and stony-iron meteorites. *Geochim. Cosmochim. Acta* **60,** 1615–1632.

Taylor G. J., Maggiore P., Scott E. R. D., Rubin A. E., and Keil K. (1987) Original structures and fragmentation and reassembly histories of asteroids: evidence from meteorites. *Icarus* **69,** 1–13.

Ulff-Møller F., Rasmussen K. L., Kallemeyn G. W., Prinz M., Palme H., and Spettel B. (1995) Differentiation of the IVA parent body: Evidence from silicate-bearing iron meteorites. *Geochim. Cosmochim. Acta* **59,** 4713–4728.

Voshage H. and Feldmann H. (1979) Investigations on cosmic-ray produced nuclides in iron meteorites, 3. Exposure ages, meteoroid sizes and sample depths determined by mass spectrometric analyses of potassium and rare gases. *Earth Planet. Sci. Lett.* **45,** 293–308.

Wasson J. T. (1974) *Meteorites.* Springer-Verlag, New York.

Wood J. A. (1979) Review of metallographic cooling rates of meteorites and a new model for the planetesimals in which they formed. In *Asteroids* (ed. T. Gehrels), pp. 849–891. Univ. Arizona Press.

Yomogida K. and Matsui T. (1984) Multiple parent bodies of ordinary chondrites. *Earth Planet. Sci. Lett.* **68,** 34–42.